Local and Global Uncertainty Analyses of a Methane Flame Model

Judit Zádor, István Gy. Zsély, and Tamás Turányi*

Department of Physical Chemistry, Eötvös University (ELTE), P.O. Box 32, H-1518 Budapest, Hungary

Marco Ratto, Stefano Tarantola, and Andrea Saltelli

Institute for the Protection and Security of the Citizen, Joint Research Centre, European Commission, 21020 Ispra (VA), Italy

Received: June 17, 2005; In Final Form: August 10, 2005

Local and global uncertainty analyses of a flat, premixed, stationary, laminar methane flame model were carried out using the Leeds methane oxidation mechanism at lean ($\varphi = 0.70$), stoichiometric ($\varphi = 1.00$), and rich ($\varphi = 1.20$) equivalence ratios. Uncertainties of laminar flame velocity, maximal flame temperature, and maximal concentrations of radicals H, O, OH, CH, and CH_2 were investigated. Global uncertainty analysis methods included the Morris method, the Monte Carlo analysis with Latin hypercube sampling, and an improved version of the Sobol' method. Assumed probability density functions (*pdf*'s) were assigned to the rate coefficients of all the 175 reactions and to the enthalpies of formation of the 37 species. The analyses provided the following answers: approximate *pdf*'s and standard deviations of the model results, minimum and maximum values of the results at any physically realistic parameter combination, and the contribution of the uncertainty of each parameter to the uncertainty of the model result. The uncertainty of a few rate parameters and a few enthalpies of formation causes most of the uncertainty of the model results. Most uncertainty comes from the inappropriate knowledge of kinetic data, but the uncertainty caused by thermodynamic data is also significant.

1. Introduction

Modeling of complex chemical kinetic systems is frequently used for obtaining scientific information that cannot be accomplished in any other way. In addition, such modeling is a common tool for the optimization of processes in chemical industry, combustion technology, and microelectronics manufacturing to improve the efficiency and to decrease the unwanted impacts on the environment. The credibility of the simulation results depends on the structure of the model, the values of the incorporated parameters, and the precision of the numerical method. Reliable chemical kinetic modeling requires the application of accurate reaction rate parameters and thermodynamic data. However, all parameters in a reaction kinetic model are results of measurements or calculations and are uncertain to some extent. Uncertainty analysis is the name of a family of mathematical methods that investigate the uncertainties of model results in light of the input uncertainties. Local uncertainty analysis utilizes the gradient of the model results in the space of parameters at the actual parameter set, whereas methods of global uncertainty analysis take into account the whole uncertainty range of parameters.

Many kinetic parameters of elementary reactions related to combustion and atmospheric chemistry have been evaluated (see, e.g., refs 1−5). These critical data evaluations not only provide the recommended kinetic parameters but also report the accuracy of the data by assigning an uncertainty factor to them. This uncertainty factor, f_j, has been defined in the following way:

$$f_j = \log_{10}\left(\frac{k_j^0}{k_j^{\min}}\right) = \log_{10}\left(\frac{k_j^{\max}}{k_j^0}\right) \quad (1)$$

where k_j^0 is the recommended value of the rate coefficient of reaction j and $k_j^{\min}$ and $k_j^{\max}$ are the extreme values; rate coefficients outside the $[k_j^{\min}, k_j^{\max}]$ interval are considered physically nonrealistic by the evaluators. Thermodynamic data compilations of gas kinetic modeling relevance[6−18] also frequently quote the variance of the enthalpy of formation of the species. There have been only a few applications of uncertainty analysis to the investigation of combustion mechanisms. The methods used by Warnatz,[19] Bromly et al.,[20] and Brown et al.[21] are variants of the local uncertainty analysis method described below, and their relation has been discussed by Turányi et al.[22] Global methods were used by Phenix et al.,[23] by Reagan et al.,[24] by Tomlin,[25] and by Zsély et al.[26] Uncertainty analysis is an often applied tool in atmospheric chemistry modeling.[27−42] These works utilize mainly global methods.

Combustion of methane is one of the most frequently modeled chemical reactions because of its high academic and industrial importance. In a recent article, Turányi et al.[22] applied local uncertainty analysis for the investigation of the effect of the uncertainty in kinetic and thermodynamic data to methane flame simulation results. The investigated model was a premixed laminar methane−air flame using the Leeds methane oxidation mechanism.[43] This mechanism contains 175 reversible reactions of 37 species. Turányi et al.[22] updated the enthalpy of formation data and assigned 1σ uncertainty values to them by processing thermodynamic data collections.[6−16] On the basis of kinetic data evaluations,[1−5] an uncertainty factor, f_j, was assigned to each rate coefficient. Assuming that the minimum and maximum

* Corresponding author. Phone: +36 1 209 0555 x 1109. Fax: +36 1 372-2592. E-mail: turanyi@elte.hu.

10.1021/jp053270i CCC: $30.25
Published on Web 10/07/2005

values of rate parameters correspond to 3σ deviations from the recommended values on a logarithmic scale, the uncertainty factor was converted to the variance of the logarithm of the rate coefficient using the following equation:

$$\sigma^2(\ln k_j) = ((f_j \ln 10)/3)^2 \tag{2}$$

In the next step, a joint kinetic and thermodynamic uncertainty analysis was carried out for several output values of the methane flame using the linear uncertainty analysis method.

A possible objection against the work of Turányi et al.[22] is the application of a linear method for the analysis of a highly nonlinear system. This linear method, to be detailed in the following section, provides exact information for linear models only, and it is expected to be applicable for nonlinear models only when the standard deviation of the parameters is sufficiently small. However, for several rate coefficients in the methane oxidation mechanism, the uncertainty factor is 1.0, that is, the corresponding rate parameter is uncertain in a range of 2 orders of magnitude.

In this paper, the methane oxidation mechanism, the reaction conditions, and the uncertainty features of the parameters were similar to those used by Turányi et al.[22] However, in this work, four different uncertainty analysis methods are utilized, which complement each other. The results not only provide a comprehensive analysis of the methane flame model but also present a cross testing of four uncertainty methods that can be used for the investigation of complex chemical kinetic models.

2. Four Methods for Uncertainty Analysis

The main task of uncertainty analysis is the determination of the probability density functions (*pdf*'s) of the model results from the joint *pdf* of the parameters. A more modest request is the calculation of the variances of model results from the variances of the parameters. The ideal method should also identify which parameters cause high uncertainty in a given model result, should determine these parameters with few calculations (using little computer time), and has to be applicable to large nonlinear models with many parameters. No such method exists, but four methods will be described in the next sections that complement each other and together provide all this information.

2.1. Linear Uncertainty Analysis. Application of linear uncertainty analysis for chemical kinetic systems has been discussed in detail by Turányi et al.[22] The basic equations are enumerated below, and some features of this method are presented here. If the rate coefficients are not correlated, then the variance of model output Y_i can be calculated in the following way:

$$\sigma_{\mathrm{K}j}{}^2(Y_i) = \left(\frac{\partial Y_i}{\partial \ln k_j}\right)^2 \sigma^2(\ln k_j) \tag{3}$$

$$\sigma_{\mathrm{K}}{}^2(Y_i) = \sum_j \sigma_{\mathrm{K}j}{}^2(Y_i) \tag{4}$$

In these equations, subscript K refers to an uncertainty of kinetic origin, $\sigma^2(\ln k_j)$ is the variance of the logarithm of rate coefficient k_j, and $(\partial Y_i/\partial \ln k_j)^2$ is the square of the seminormalized local sensitivity coefficient. Partial variance $\sigma_{\mathrm{K}j}{}^2(Y_i)$ is the contribution of the uncertainty of the rate coefficient of reaction j to the variance of model output Y_i. If the model were linear, then the kinetic uncertainty contribution $\sigma_{\mathrm{K}}{}^2(Y_i)$ would be the exact variance of Y_i because of the uncertainty of kinetic parameters. $S_{\mathrm{K}}\%_{ij}$ indicates the percentage contribution of $\sigma_{\mathrm{K}j}{}^2(Y_i)$ to $\sigma_{\mathrm{K}}{}^2(Y_i)$.

The influence of the enthalpy of formation data on the model result can be calculated in a similar way, assuming that the data are uncorrelated:

$$\sigma_{\mathrm{T}j}{}^2(Y_i) = \left(\frac{\partial Y_i}{\partial \Delta_{\mathrm{f}} H^\circ_{298}(j)}\right)^2 \sigma^2(\Delta_{\mathrm{f}} H^\circ_{298}(j)) \tag{5}$$

$$\sigma_{\mathrm{T}}{}^2(Y_i) = \sum_j \sigma_{\mathrm{T}j}{}^2(Y_i) \tag{6}$$

where subscript T refers to thermodynamic uncertainty; $\partial Y_i/\partial \Delta_{\mathrm{f}} H^\circ_{298}(j)$ is the local enthalpy of formation sensitivity coefficient, which is a linear estimation of the effect of changing the enthalpy of formation; and $\sigma_{\mathrm{T}}{}^2(Y_i)$ is the variance of model output Y_i due to the uncertainties of the enthalpies of formation of all species. The partial thermodynamic uncertainty contribution $\sigma_{\mathrm{T}j}{}^2(Y_i)$ is the contribution of the uncertainty of the enthalpy of formation of species j to the variance of model output Y_i, and $S_{\mathrm{T}}\%_{ij}$ indicates the percentage contribution of $\sigma_{\mathrm{T}j}{}^2(Y_i)$ to $\sigma_{\mathrm{T}}{}^2(Y_i)$.

The kinetic and thermodynamic parameters are assumed to be uncorrelated; therefore, the sum of the variances of kinetic and thermodynamic origin provides the variance of the model result:

$$\sigma^2(Y_i) = \sigma_{\mathrm{K}}{}^2(Y_i) + \sigma_{\mathrm{T}}{}^2(Y_i) \tag{7}$$

We can also calculate the values

$$S\%_{ij} = \frac{\sigma_j{}^2(Y_i)}{\sigma^2(Y_i)} \times 100\% \tag{8}$$

where $\sigma_j{}^2(Y_i)$ is either of kinetic or of thermodynamic origin.

Partial variances $\sigma_{\mathrm{K}j}{}^2(Y_i)$ and $\sigma_{\mathrm{T}j}{}^2(Y_i)$ and the percentage contribution of their sum to the variances indicate the share of the uncertainty of parameter j to the uncertainty of result i. Most of the simulation programs in reaction kinetics include built-in routines to calculate local sensitivity coefficients; therefore, the variances and uncertainty contributions above can be easily calculated. The drawback of this method is that the calculated values are local estimates only, and the accuracy of this approximation cannot be assessed.

2.2. Monte Carlo Analysis with Latin Hypercube Sampling. In the Monte Carlo (MC) analysis,[44] a large number of parameter sets are generated according to the probability density functions of the parameters. The model is simulated with each of these parameter sets, and the results are processed with statistical methods. The cornerstone of this approach is the application of an efficient and unbiased method for the selection of the parameter sets. In Latin hypercube sampling,[44] the range of parameters to be varied during the MC simulations is divided into intervals of equal probability. The parameter values are then randomly and independently sampled in each interval, and the selected values of the parameters are randomly grouped without repetition. This ensures that the parameter space is represented with a good approximation of full coverage. Analysis of the MC simulation results included the calculation of the means and the variances of the model output, as well as the investigation of the resulting *pdf*'s. Monte Carlo analysis frequently requires several thousand runs of the model but provides accurate and unbiased information about the uncertainty of model results. Although it is possible to calculate individual

contributions of the parameters to the uncertainty of the output values, e.g., via standardized regression coefficients,[44] determination of accurate values requires far too many calculations with this method.

2.3. The Morris Method. The Morris one-at-a-time (MOAT) method[44,45] is a global technique, which also estimates the contribution of the parameters to the uncertainty of the results. $N + 1$ parameter sets are designed (where N is the number of parameters) with the algorithm of Morris, so that a given parameter takes exactly two values throughout the sets: in every run, exactly one parameter is changed randomly compared to the previous run, and every parameter is changed exactly once during the $N + 1$ runs. The values of the parameters are selected from the whole range of the parameter values by setting out m equidistant points. A higher m value implies a finer grid, and m is usually recommended to be around 5; this is the value that we used. Because MOAT is a screening method (i.e., the results are qualitative), increasing the value of m does not cause significant change in the results. The procedure is repeated several times, so new $N + 1$ parameter sets are designed in the same way.

The elementary effect d_{ij} of parameter p_j on output value Y_i can be calculated in the following way:

$$d_{ij} = |Y_i(p_1, ..., p_{j-1}, p_j \pm \Delta, p_{j+1}, ..., p_N) - Y_i(p_1, ..., p_{j-1}, p_j, p_{j+1}, ..., p_N)| \quad (9)$$

where p_1, p_2, etc. are either the kinetic or the thermodynamic parameters and Δ is a step size given by the algorithm, with which parameter p_j is changed. Equation 9 is calculated for all the $N + 1$ runs, and it gives one effect value of d_{ij} per run per output variable. Calculating d_{ij} several times using different parameter sets, the means and the standard deviations of the effects are plotted against each other. Parameters with a high mean effect are influential, whereas a low mean effect shows that uncertainty in that parameter does not affect the given output variable significantly. Low standard deviation shows that the parameter has approximately a linear effect, whereas a high value means that the effect of that parameter is nonlinear or very much depends on the actual values of the other parameters (interaction). The output of the Morris method is a graph showing the standard deviation of each parameter effect vs their mean effect. Unimportant parameters are in the bottom left corner, important parameters with linear effects are in the lower right region, and parameters with nonlinear or interaction effects are in the top right region of the graph. In the original work of Morris,[45] eq 9 was used without taking the absolute values. As has been shown by Campolongo et al.,[46] using the absolute value of the deviations is a more appropriate way to rank factors in the order of importance.

The advantage of the Morris method is its computational cheapness, while the parameters are varied in their whole range. In addition, the effect of a parameter is calculated at randomly selected values of the other parameters. However, it does not take into account the probability distribution functions of the parameters. In our calculations, every parameter could take four equidistant values (minimum, maximum, and two intermediate values) and the procedure was repeated 10 times ($10 \times (N + 1)$ runs in total).

2.4. Sensitivity Indices. The fourth method employed in this work is a further developed version[47] of the Sobol'[48] method. This is a global sensitivity analysis method, which quantitatively gives the relative importance of input variable p_j in determining the value of an output variable $Y_i = f_i(p_1, p_2, ..., p_N)$. If the joint probability of the input is $P(p_1, p_2, ..., p_N)$, the variance of output Y_i can be expressed as

$$V(Y_i) = \int\int ... \int f_i^2(p_1, p_2, ..., p_N)\, P(p_1, p_2, ..., p_N)\, dp_1\, dp_2 ... dp_N - E^2(Y_i) \quad (10)$$

where $E(Y_i)$ is the mean value of the output Y_i. To get the variance in Y_i due to all parameters but p_j, the calculation of the above integral is needed at fixed values of p_j, for which the $V(Y_i|p_j = \tilde{p}_j)$ notation is used. Taking all possible $\tilde{p}_j$ values into account, the mean $E(V(Y_i|p_j))$ of these values can be obtained. Then, the difference $V(Y_i) - E(V(Y_i|p_j))$ gives the variance of the expected value of Y_i due to p_j only, $V(E(Y_i|p_j))$. From this, the first-order sensitivity indices (that is, the main effect) can be calculated:

$$S_{j(i)} = V(E(Y_i|p_j))/V(Y_i) \quad (11)$$

which characterizes the contribution of parameter p_j to the variance of the output variable Y_i when the effects of the other parameters are taken on average. The first-order indices are scaled between 0 and 1.

If the input parameters are uncorrelated, it is possible to repeat the procedure by fixing two parameters at a time. The resulting values are the second-order sensitivity indices:

$$S_{kj(i)} = \frac{V(E(Y_i|p_k, p_j)) - V(E(Y_i|p_k)) - V(E(Y_i|p_j))}{V(Y_i)} \qquad k \neq j \quad (12)$$

The second-order term accounts for the variation in Y_i that cannot be explained by p_i and p_k alone (that is the interaction of parameters). Higher-order terms can be constructed in a similar way.

The total effect of a parameter ($S^{tot}_{j(i)}$) is the sum of all terms related to the uncertainty contribution of output value Y_i, which contain parameter j. For example, if there are three parameters (denoted by a, b, and c), then

$$S^{tot}_{a(i)} = S_{a(i)} + S_{ab(i)} + S_{ac(i)} + S_{abc(i)} \quad (13)$$

The total effect is a very useful measure of nonadditivity in a model. For a purely additive model $\sum_{j=1}^{N} S_{j(i)} = 1$. On the other hand, for a model with interacting parameters, the difference $S^{tot}_{j(i)} - S_{j(i)}$ shows the level of interactions, which can be further investigated through the second-order terms $S_{kj(i)}$.

For the computation of sensitivity indices, several methods have been developed, such as the method of Sobol'[48] or the extended version of the Fourier Amplitude Sensitivity Test (FAST).[49] In this work, the method of Saltelli is used,[47] which is an extended version of the Sobol' method. The method requires $M(2N + 2)$ number of Monte Carlo runs in a designed fashion and provides $S_{j(i)}$, $S^{tot}_{j(i)}$, and $S_{kj(i)}$; increasing the number of repetitions, M, increases the accuracy of the method. This method is cheaper and more efficient than the original Sobol' method and the extended FAST.

3. Uncertainty Analysis of a Methane Flame Model

Using the uncertainty analysis methods described in the previous section, we examined the Leeds methane oxidation mechanism[43] at the conditions of a one-dimensional (i.e., flat), adiabatic, freely propagating, laminar, premixed flame. The

mechanism contains 175 reactions of 37 species, which also implies 37 enthalpies of formation data. The enthalpy of formation of species H_2, O_2, and N_2 is zero at 298.15 K by definition, and the associated uncertainty is also zero. The remaining 34 species have an enthalpy of formation with nonzero uncertainties at 298.15 K. This means that the total number of parameters to be investigated was 209. The cold boundary conditions were $p = 1.0$ atm and $T_c = 298.15$ K. The investigated mechanism, the modeling conditions, and the uncertainty features of the parameters were identical with those used in the article of Turányi et al.,[22] with the following exceptions. Application of global methods requires not only the mean and the variance of the parameters but also their *pdf*'s. The assumed variances of the parameters were identical with those used in the article,[22] and normal distribution truncated at $\pm 3\sigma$ was assumed for parameters ln k_j and $\Delta_f H^\circ_{298}(j)$, i.e., the minimum and maximum values of these parameters were $p_j^0 - 3\sigma(p_j)$ and $p_j^0 + 3\sigma(p_j)$, respectively. This is in accordance with the assumed extremes of rate coefficients as usually defined in the kinetic evaluations (see eqs 1 and 2); the possible extremes of the enthalpy of formation data were defined in an analogous way. The uncertainty factors f_j assigned to each reaction step can be downloaded from our Web site,[43] and the variance of the enthalpies of formation can be found in Table 1 in the article by Turányi et al.[22]

In the previous work,[22] the methane flame was investigated at equivalence ratios $\varphi = 0.62$, $\varphi = 1.00$, and $\varphi = 1.20$. The lean equivalence ratio $\varphi = 0.62$ is close to the low extinction limit. Therefore, in the global uncertainty calculations in the cases of several parameter sets, it was not possible to model a propagating flame; hence, it was not possible to interpret quantitatively the simulation results. Therefore, a slightly richer mixture of $\varphi = 0.70$ was chosen in the present calculations, which resulted in a more stable flame that was not simulated to be extinguished at any of the parameter sets.

At the time of the publication of the article,[22] the enthalpy of formation of OH was debated and therefore all calculations were done twice, assuming a higher variance of 2.1 kJ mol^{-1} and a lower variance of 0.38 kJ mol^{-1} for $\Delta_f H^\circ_{298}$(OH). The former reflected the scatter of the $\Delta_f H^\circ_{298}$(OH) values found in the literature, and the latter was the new recommendation by Ruscic et al.[50,51] Recently, the enthalpy of formation of OH and its uncertainty as recommended by Ruscic et al.[51] became generally accepted; therefore, in this work, only the lower variance of 0.38 kJ mol^{-1} for $\Delta_f H^\circ_{298}$(OH) was considered.

In the work of Turányi et al.,[22] the kinetic and thermodynamic uncertainties were calculated separately and these results were merged only in the last step. The calculated thermodynamic uncertainties were accurate; however, because of a program error, the kinetic uncertainties were somewhat smaller, and their relative magnitudes were also not accurate. This resulted in the results, given in Table 2 and Figure 2 of that article,[22] being incorrect, although they are in most cases qualitatively true. Figure 1 of the article[22] shows that the ratio of kinetic and thermodynamic uncertainties is also flawed, demonstrating an exaggerated effect of thermodynamic uncertainties. In this article, the correct local uncertainty results and the correct ratio of kinetic and thermodynamic uncertainties are published. This time, it was possible to check the local uncertainty results by comparing them with the Monte Carlo outcomes. Another, less significant error was also found in the same article:[22] the recommended enthalpy of formation of C_3H_2 is 476.95 kJ mol^{-1} instead of 591.71 kJ mol^{-1} as indicated in column 2 of Table 1. During the calculations reported,[22] the former value was used.

Methane flame models produce a large number of numerical results, but only some important ones were selected to make the uncertainty analysis effective. In accordance with the previous article,[22] the following model outputs were considered: laminar flame velocity v_L, maximum flame temperature T_{max}, and maximum concentrations of radicals H, O, OH, CH, and CH_2. These quantities are generally accepted important features of a methane flame. Reproduction of the experimental laminar flame velocity is a usual test of combustion mechanisms. Exact calculation of the H atom concentration is of high importance because this radical is the most effective chain carrier in hydrocarbon combustion systems. Exact calculation of the flame temperature is also important because a possible aim of combustion calculations is the determination of heat release. Another usual aim of combustion simulations is the calculation of NO production. NO generation is determined by the local temperature and the concentration of radicals O and OH via the extended Zeldovich mechanism. In the Fenimore mechanism of NO generation and at reburn conditions, the NO production is controlled to a great extent by the concentration of radicals CH and CH_2.

For the flame simulations, the PREMIX code[52] was used, and the local sensitivities were converted to uncertainty features using the program KINALC.[53] The MOAT, the LHS Monte Carlo, and the improved Sobol' methods were carried out using purpose written codes. A single simulation of the methane flame model from good starting conditions required 30−40 s on a 2000 MHz PC, and the local sensitivity analysis required additionally about the same time. Calculations with certain parameter sets required significantly more time (up to 10 min each). The Morris method and the Monte Carlo analysis required 2130 and 3000 runs, respectively, for each equivalence ratio. The Sobol' method, which allows us to estimate first-, second-, and total-order terms has a cost of $M(2N + 2) = 220(2 \times 36 + 2) = 13\,640$ (N is the number of investigated parameters). Application of these three methods required approximately 22, 33, and 167 h of computational time, respectively, for each equivalence ratio.

3.1. Uncertainty of Model Results. Results of any mathematical model are determined by the structure of the model, the parameters used, and the method of the solution. The governing partial differential equations of a one-dimensional stationary flame model and the applied numerical methods are well established. Also, the stoichiometry of the reaction steps of methane oxidation is widely accepted (see an analysis in Hughes et al.[54]), and all current methane oxidation mechanisms use a very similar set of reactions. The largest uncertainty is in the values of the parameters, but as described above, realistic estimations of the uncertainty bounds for all parameters are available.

Monte Carlo analysis is the best method for the determination of the uncertainty of model results. Table 1 contains the monitored simulation results at the nominal set of parameters along with their standard deviations (also expressed in percentages) as determined by the Monte Carlo analysis. This table also contains these values as determined by local uncertainty analysis. Table 1 shows that in all cases there is a fairly good agreement between the Monte Carlo and the local uncertainty analysis results. However, it is important to note that the 1σ uncertainty of the laminar flame velocity is consistently underpredicted by approximately 1−2 cm s^{-1} in the local analysis at all fuel/air ratios.

Precise determination of the extremes of the results would require a sophisticated parameter estimation task with a very

TABLE 1: Simulation Results at the Original Parameter Set, Standard Deviation (1σ) of the Results Determined by Local Uncertainty, and Monte Carlo Analyses[a]

	nominal values	local analysis standard deviation		Monte Carlo analysis					
				standard deviation		minimum		maximum	
		1σ	%	1σ	%	value	%	value	%
				$\varphi = 0.70$					
v_L/cm s^{-1}	21.64	2.95	13.6	4.05	19.1	9.95	47.0	36.22	171.2
T_{max}/K	1806.46	8.62	0.5	10.36	0.6	1751.39	97.0	1828.49	101.3
$w_{H,max}/10^{-5}$	5.82	1.57	27.1	1.40	25.0	2.00	35.8	10.70	191.5
$w_{O,max}/10^{-3}$	1.33	0.20	15.3	0.23	17.9	0.60	46.5	2.04	159.4
$w_{OH,max}/10^{-3}$	2.85	0.23	8.2	0.26	9.2	1.85	66.3	3.60	129.0
$w_{CH,max}/10^{-8}$	2.94	1.89	64.7	1.77	59.7	0.35	11.8	16.80	567.1
$w_{CH_2,max}/10^{-6}$	3.61	1.32	36.6	1.09	32.8	0.79	23.6	9.11	273.4
				$\varphi = 1.00$					
v_L/cm s^{-1}	38.11	4.57	12.0	6.17	16.4	21.31	56.6	61.56	163.4
T_{max}/K	2224.23	2.82	0.1	1.73	0.1	2217.36	99.7	2228.58	100.2
$w_{H,max}/10^{-4}$	2.14	0.31	14.7	0.26	12.6	1.31	63.1	2.99	144.4
$w_{O,max}/10^{-3}$	1.74	0.23	13.3	0.18	10.4	1.13	66.9	2.30	136.1
$w_{OH,max}/10^{-3}$	5.27	0.19	3.6	0.21	4.0	4.50	86.4	5.98	114.8
$w_{CH,max}/10^{-7}$	8.07	3.74	46.3	3.73	49.2	1.18	15.5	36.00	474.6
$w_{CH_2,max}/10^{-5}$	2.54	0.60	23.8	0.56	24.0	0.89	37.9	5.15	219.5
				$\varphi = 1.20$					
v_L/cm s^{-1}	27.22	5.23	19.2	6.70	24.2	10.05	36.3	53.80	194.1
T_{max}/K	2131.82	3.72	0.2	4.74	0.2	2092.03	98.2	2136.61	100.3
$w_{H,max}/10^{-4}$	2.10	0.48	23.0	0.34	16.3	0.91	43.6	3.21	153.6
$w_{O,max}/10^{-4}$	4.05	1.75	43.2	1.29	30.9	0.83	19.9	8.82	212.0
$w_{OH,max}/10^{-3}$	2.97	0.49	16.6	0.42	14.3	1.38	46.8	4.19	142.0
$w_{CH,max}/10^{-6}$	2.61	0.99	37.7	0.97	42.3	0.56	24.3	8.55	369.9
$w_{CH_2,max}/10^{-5}$	3.68	1.22	33.2	0.85	24.7	1.36	39.5	7.45	216.3

[a] Minimum and maximum values are determined by the Monte Carlo analysis. All values are also expressed as a percentage of the nominal values.

large number of simultaneously changed parameters. For example, in the present model, the values of 209 parameters should be optimized, which is a very challenging problem. During the Latin hypercube Monte Carlo analysis, all parameters are changed simultaneously and these parameter sets have been designed to cover the whole parameter space. Therefore, the minimum and maximum values collected from the Monte Carlo analysis results provide a good estimation of the attainable minimum and maximum model answers. Calculation of these extreme values is very important. If the experimental data lie outside the range of attainable results, then the structure of the model is surely wrong (e.g., important reactions are missing), provided that the *pdf*'s of the parameters have been estimated correctly. Table 1 contains the minimum and maximum values of the model results and their percentage relation to the main value.

The standard deviation of the calculated flame velocity $\sigma(v_L)$ is 4.1 cm s^{-1}, 6.2 cm s^{-1}, and 6.7 cm s^{-1} for lean ($\varphi = 0.70$), stoichiometric ($\varphi = 1.00$), and rich ($\varphi = 1.20$) flames, respectively. These are 19.1%, 16.4%, and 24.2% of the nominal values, respectively. The experimental uncertainty of the determination[55] of laminar flame velocity is about ± 1 cm s^{-1}. Methane flame models using the most recent reaction mechanisms usually also reproduce[54] the experimental data within ± 1 cm s^{-1}. Such an accuracy can be achieved only by chance or by fine-tuning of the parameters because the intrinsic uncertainty of the models is on the order of $\pm 4-7$ cm s^{-1} at the 1σ level, according to the present study. Tuning the parameters within the physically realistic limits, the laminar flame velocity can be changed significantly. For example, in the case of stoichiometric flame, the laminar flame velocity can be tuned between 21 and 62 cm s^{-1}.

On the other hand, the flame temperature is calculated very precisely by the models. For example, in the stoichiometric case, the standard deviation of the maximum flame temperature is 1.7 K at the 1σ level and the achievable values deviate from the nominal value only by 5−7 K. The very low uncertainty (0.1−0.5%) of the calculated temperature is reassuring. The main reason for this is that the calculated maximum temperature depends mainly on the enthalpies of formation of CH_4, H_2O, CO_2, and CO, and these values are known with very low uncertainty.

The standard deviations of the calculated maximum radical concentrations are in the 4−60% range of the nominal values, and they depend on the fuel/air ratio. In general, the standard deviations of O, H, and OH are relatively low, and those of CH and CH_2 are high. This means that the calculation of the prompt NO production cannot be performed with high accuracy, even if the parameters of the nitrogen reactions were known with low uncertainty.

Another result of the Monte Carlo analysis is the *pdf*'s of the output values through the analysis of histograms and cumulative distribution functions. Some typical examples are shown in Figure 1. The maximum temperature is limited by the adiabatic thermodynamic threshold value; this limiting value cannot be exceeded using any kinetic parameter set, and modifications of the kinetic parameters may lower the calculated temperature peak. This is probably the reason the temperature histogram is steep toward the high temperatures and has a long tail toward the low temperatures. This behavior is the most emphasized in the rich flame (Figure 1c), but also characteristic for the lean and the stoichiometric flames (Figure 1a,b).

For the flame velocity and the concentrations of species, the physical upper limits are not close to the calculated values obtained by the original parameter set and the histograms of these results are different (see Figure 1d−f). The calculated OH atom concentration is nearly of normal distribution (see Figure 1e), and similar patterns were obtained for the distribution of the flame velocity and the concentrations of O and H at all the three equivalence ratios investigated. The calculated CH

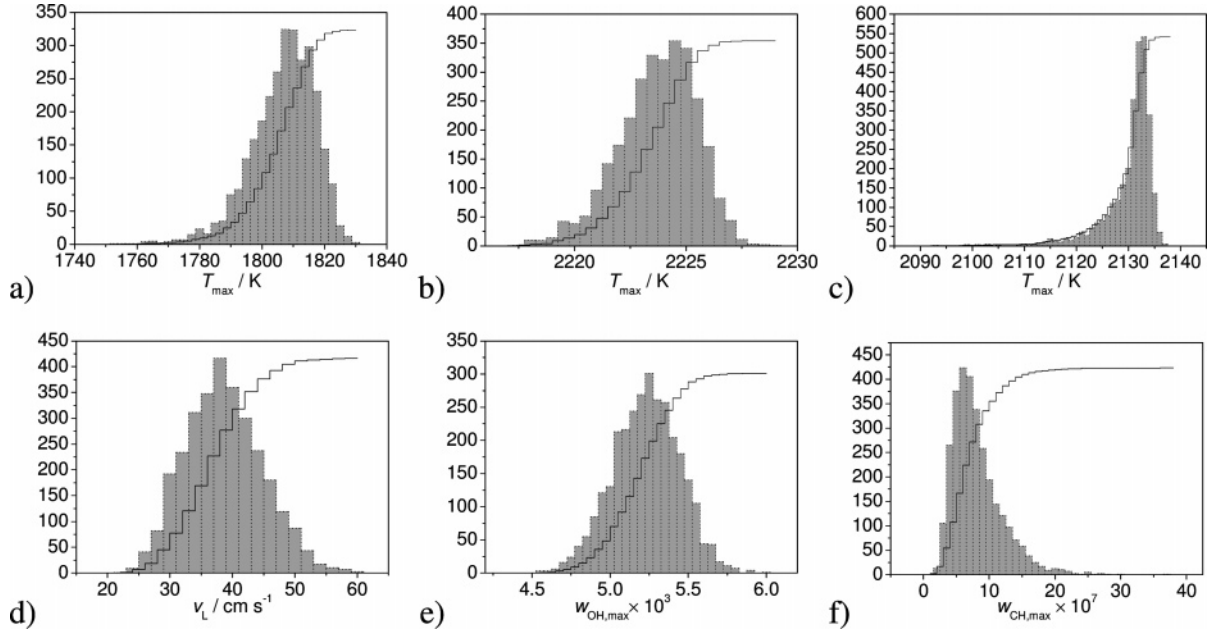

Figure 1. Histograms and empirical cumulative distribution functions of some selected model outputs: (a) maximum temperature at $\varphi = 0.70$, (b) maximum temperature at $\varphi = 1.0$, (c) maximum temperature at $\varphi = 1.20$, (d) laminar flame velocity at $\varphi = 1.0$, (e) maximum OH concentration at $\varphi = 1.0$, and (f) maximum CH concentration at $\varphi = 1.0$.

radical concentrations have a longer tail to the direction of higher values (see Figure 1f), and similar histograms were obtained for radical CH_2, also in the whole range of equivalence ratios.

3.2. Tracing the Origin of Uncertainty. The influence of the uncertainty of the thermodynamic and kinetic parameters on the uncertainty of each model result was contrasted in Figure 2 (see upper bars) by comparing the extent of the terms σ_K^2 and σ_T^2 of eq 7, calculated by local uncertainty analysis. The lower bars in this figure refer to the ratio of the sum of the first-order Sobol' indices, related to kinetic and thermodynamic parameters. Despite the basic difference in these methods, there is an excellent agreement among their results. Uncertainty in the maximum temperature at stoichiometric conditions is highly related to the thermodynamic uncertainties. The calculated concentration of the OH radical is also sensitive to uncertainties in the thermodynamic parameters, mainly at lean and stoichiometric conditions. The overall contribution of thermodynamic parameters to the uncertainty of the results is less significant than that of the kinetic parameters, but these are in the range of 3−10% and thus certainly can not be neglected.

In Figure 3, some of the Morris plots are presented. In these plots, all points, which are clearly distinct from the really unimportant ones, were marked, without selecting a uniform threshold value for the mean or for the variance of the effect of the outputs to be shown. In Figure 3a,c,e, the Morris plots for the laminar flame velocity are shown at different equivalence ratios. Reaction $O_2 + H = OH + O$ has the greatest contribution in the uncertainty, and reactions $CO + OH = CO_2 + H$ and $HCO + M = H + CO + M$ also have a great effect. It can be seen that reaction $O_2 + H = OH + O$ has a smaller variance/mean ratio than the other reactions.

The Morris analysis indicates that the uncertainty of the enthalpy of formation of the OH radical is a major source of the uncertainty of the maximum OH concentration for all equivalence ratios and also shows that this influence is nearly linear. The termolecular reaction of $O_2 + H + M$ and that of $H + OH + M$ also has a relatively low nonlinear effect on the maximal OH concentration. In general, it can be seen that the nonlinear effects cannot be neglected to achieve a realistic order of importance of the parameters.

In the local uncertainty analysis, it is possible to calculate the percentage contributions of the individual input parameters to the output values (see eq 8). Figure 4 shows the percentage contributions for all monitored variables in the cases of lean, stoichiometric, and rich flames. These speck figures have been constructed in such a way that the monitored variables are aligned on the horizontal axis, and the input parameters are along the vertical axis; the magnitude of the uncertainty contribution is reflected in the thickness of the specks (continuous scale). Only parameters with at least 1% contribution are shown. Blank areas mean that a given parameter has less than 1% contribution in that case to the uncertainty of a monitored output.

The number of reactions causing high uncertainty is around 30 in every case, which is approximately one-sixth of the total number of reactions. Moreover, there are only a few really major sources of uncertainty at all equivalence ratios.

For the efficient calculation of the sensitivity indices, it was crucial to reduce the total number of varied parameters because treating all parameters as uncertain ones would have required too long of a computational time. To stay on the safe side, a parameter was selected if it was found to be important for at least one result either in the local or in the Morris analysis. A group of 27−32 parameters of the possible 209 parameters were selected at each equivalence ratio for the calculation of the Sobol' indices. The first-order sensitivity indices are shown in Figure 5, but only for parameters having $S_{j(i)} > 0.01$. The representation of the data is the same as for the results of the local analysis (Figure 4), to facilitate comparison. The sums of the first-order indices are also shown in the bottom of the columns. It should be noted that, although the local uncertainty contributions always add up to 100% by definition, the sum of the first-order sensitivity indices could be lower if higher-order effects play an important role. However, the calculation of the first-order indices has some numerical inaccuracy, so for values close to 100, it is adequate to say that there are not any important higher-order effects.

Comparison of Figures 4 and 5 indicates that the local uncertainty analysis and the calculation of uncertainty indices gave qualitatively the same results, and the agreement is almost quantitative. For example, in the stoichiometric case (Figure

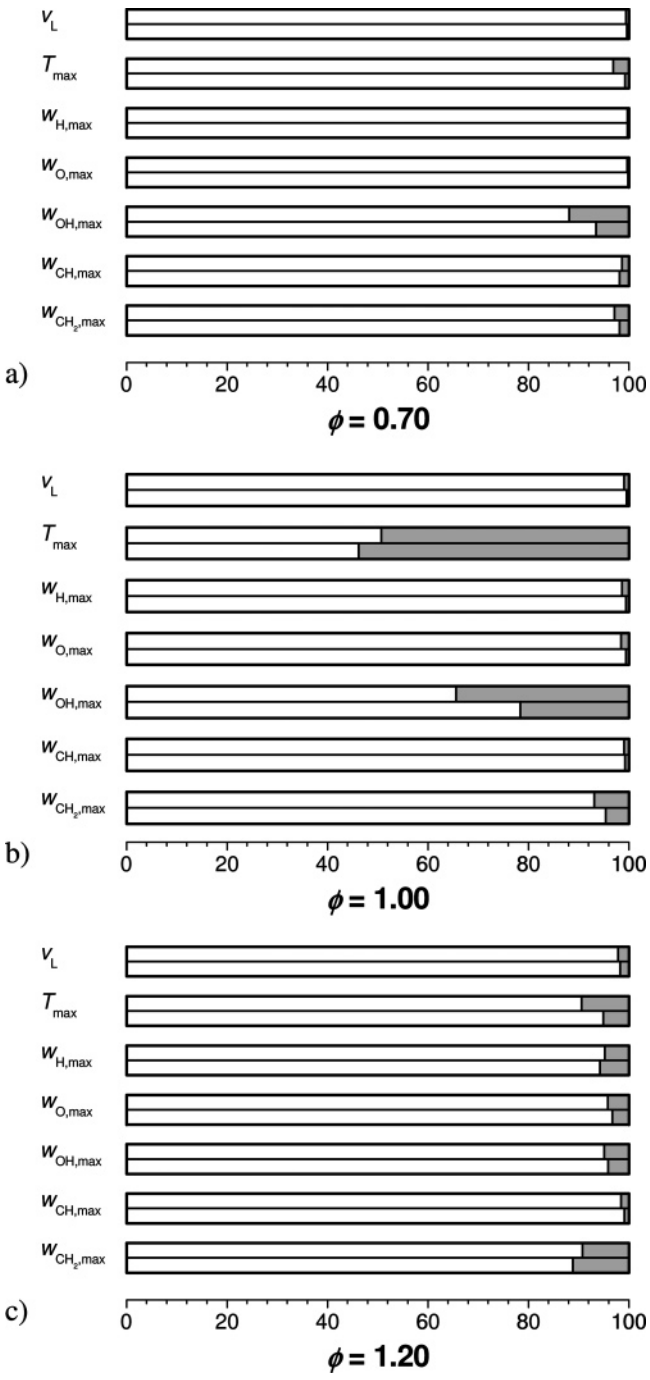

Figure 2. Kinetic (white) and thermodynamic (gray) contributions to the total uncertainty of the monitored parameters calculated by local uncertainty analysis (upper bars) and by the Sobol' method (lower bars) expressed as percentages. Results for (a) lean, (b) stoichiometric, and (c) rich flames are shown.

5b), there are only minor differences between the results of the local analysis and the sensitivity indices. The relative importance of the $O_2 + H = OH + O$ reaction seems to be slightly lower, and those of the thermodynamic parameters are higher. For the rich flame, there are more significant differences between the findings of the two methods. According to the local analysis, the $H + CH_3 (+ M) = CH_4 (+ M)$ reaction is important for all variables, but CH. This observation is not in complete agreement with the sensitivity indices, where this reaction has only a secondary importance. Because the extended Sobol' method is more sophisticated and general than the local uncertainty analysis, in the next paragraphs, the influence of the kinetic and thermodynamic parameters on the modeled results will be discussed on the basis of sensitivity indices (see Figure 5).

The reaction of O_2 with H is one of the most important reactions; the bimolecular $O_2 + H = OH + O$ reaction channel dominates as the main contributor to the uncertainty of the monitored variables. This contribution is very high in several cases; for example, in the rich mixture, this gives more than 70% of the uncertainty of T_{max} and v_L; and in the stoichiometric case, it is responsible for more than 80% of the T_{max} uncertainty. In the lean case, the other important reaction is the $CO + OH = CO_2 + H$ reaction, which also contributes largely (10−30%) to output uncertainties. The most important reaction for CH_2 is $CH_3 + OH = CH_2(s) + H_2O$ in the lean case (∼30%), but its dominance is overridden by the $O_2 + H = OH + O$ reaction in the rich case. The relaxation of the singlet CH_2 radical to the ground state does not cause much uncertainty to the CH_2 concentration (5−10%). The greatest contribution to the $w_{CH,max}$ uncertainty is due to the $H + CH_2 = CH + H_2$ reaction; in the lean flame, it has about a 20% share, and in the rich case, it has about 30%. Another important contributor to CH uncertainty is the $C_2H_2 + OH = C_2H + H_2O$ reaction, having about 10−20% contribution in all cases. The contributions to the uncertainty of T_{max} show an interesting pattern. First, the number of important contributors decreases with increasing equivalence ratio, enumerating 16, 13, and 9 in the lean, stoichiometric, and rich cases, respectively. Also, the share of the most important parameters is different at different fuel/air ratios: in the lean case, $C_2H_4 + O = H + CH_2HCO$ has ∼25%; in the stoichiometric case, the enthalpy of formation of CH_2CHO has ∼35%; and in the rich case, the $O_2 + H = OH + O$ reaction has ∼70%. This variability is interesting because T_{max} is the model result that has the lowest uncertainty (see Table 1).

Several thermodynamic input parameters were also found to be influential. Although the relative uncertainty in the enthalpy of formation of the OH radical is small, it still plays a significant part in the resulting $w_{OH,max}$ uncertainty in the lean and stoichiometric cases; in the stoichiometric case, it is responsible for approximately 30% of the calculated uncertainty. The CH_2-CO radical contributes greatly to the T_{max} uncertainty in the stoichiometric case. Other important thermodynamic parameters are the enthalpies of formation of CH_4, CH_2OH, $CH_2(S)$, and CH_2; the latter two are important only in the uncertainty of the CH_2 radical concentration.

In the lean case, the model is fairly additive for all the outputs but CH, where all the factors, taken on their own, explain only 70% of the total variance of CH. This 70% is mainly due to reaction $H + CH_2 = CH + H_2$ (18%), reaction $C_2H_2 + OH = C_2H + H_2O$ (13%), reaction $CO + OH = CO_2 + H$ (10%), and reaction $O_2 + CH = CO + OH$ (9%). The remaining 30% is due to interactions among the parameters. To find the higher-order interactions for each parameter, the differences between their total indices $S_{j(i)}^{tot}$ and their first-order indices $S_{j(i)}$ should be considered. This analysis has shown that second- and higher-order effects also originate from the main contributors listed above. Calculating the second-order indices, we obtained the following results: the interaction of $C_2H_2 + OH$ and $CO + OH$ accounts for 16% of the total variance of CH, the interaction of $C_2H_2 + OH$ and $O_2 + CH$ accounts for 9%, the interaction of $H + CH_2$ and $CO + OH$ accounts for 6%, and the interaction of $H + CH_2$ and $C_2H_2 + OH$ accounts for 5%. This explains the missing part of the variance of CH concentration in the lean case; no third-order parameter interactions have to be taken into account.

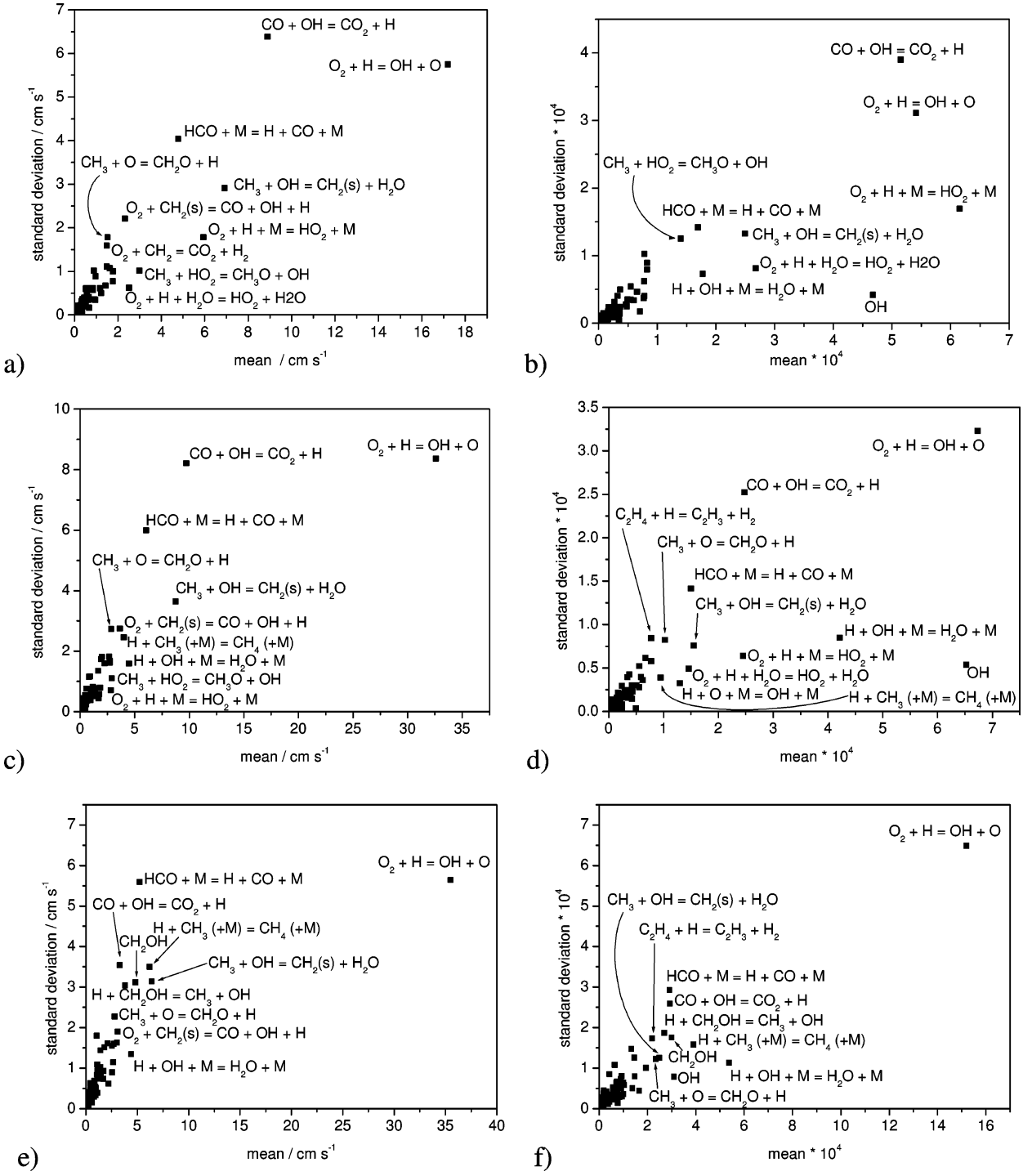

Figure 3. Morris plots for (a) laminar flame velocity at $\varphi = 0.7$, (b) maximum OH concentration at $\varphi = 0.7$, (c) laminar flame velocity at $\varphi = 1.0$, (d) maximum OH concentration at $\varphi = 1.0$, (e) laminar flame velocity at $\varphi = 1.20$, and (f) maximum OH concentration at $\varphi = 1.20$.

For stoichiometric and rich methane flames, first-order indices add up to ~100%, but in some cases, the deviation from 100% is around ±10%. To see whether it is due to numerical instabilities or to higher-order effects, the difference between the total and the first-order indices for each parameter has to be inspected. For all monitored variables but the maximum concentration of CH, these differences are minor; therefore, second- and higher-order effects are not significant for these variables. Second-order effects, i.e., interactions of pairs of parameters, were calculated in the case of CH. In the stoichiometric flame, the interaction of reactions $C_2H_2 + OH = C_2H + H_2O$ and $H + CH_2 = CH + H_2$ explains the entire difference between the total and the first-order indices. In the rich flame, the interaction of the two main contributors, reactions $O_2 + H = OH + O$ and $H + CH_2 = CH + H_2$, does not account for the missing variance. We have found that the interaction of reactions $C_2H_2 + CH = C_2H + CH_2$ and $C_2H_2 + OH = C_2H + H_2O$ accounts for 3% of the missing variance; the rest is due to third- and higher-order effects, which were not investigated.

3.3. Monte Carlo Analysis of Local Sensitivity Coefficients. When presenting results of a local sensitivity analysis for nonlinear models, it is always emphasized[56] that they are valid only at the nominal values of the parameters. Using the MC analysis, it is possible to carry out local sensitivity analysis systematically at other sets of the parameters. Therefore, during the MC simulations, the first-order local sensitivity coefficients

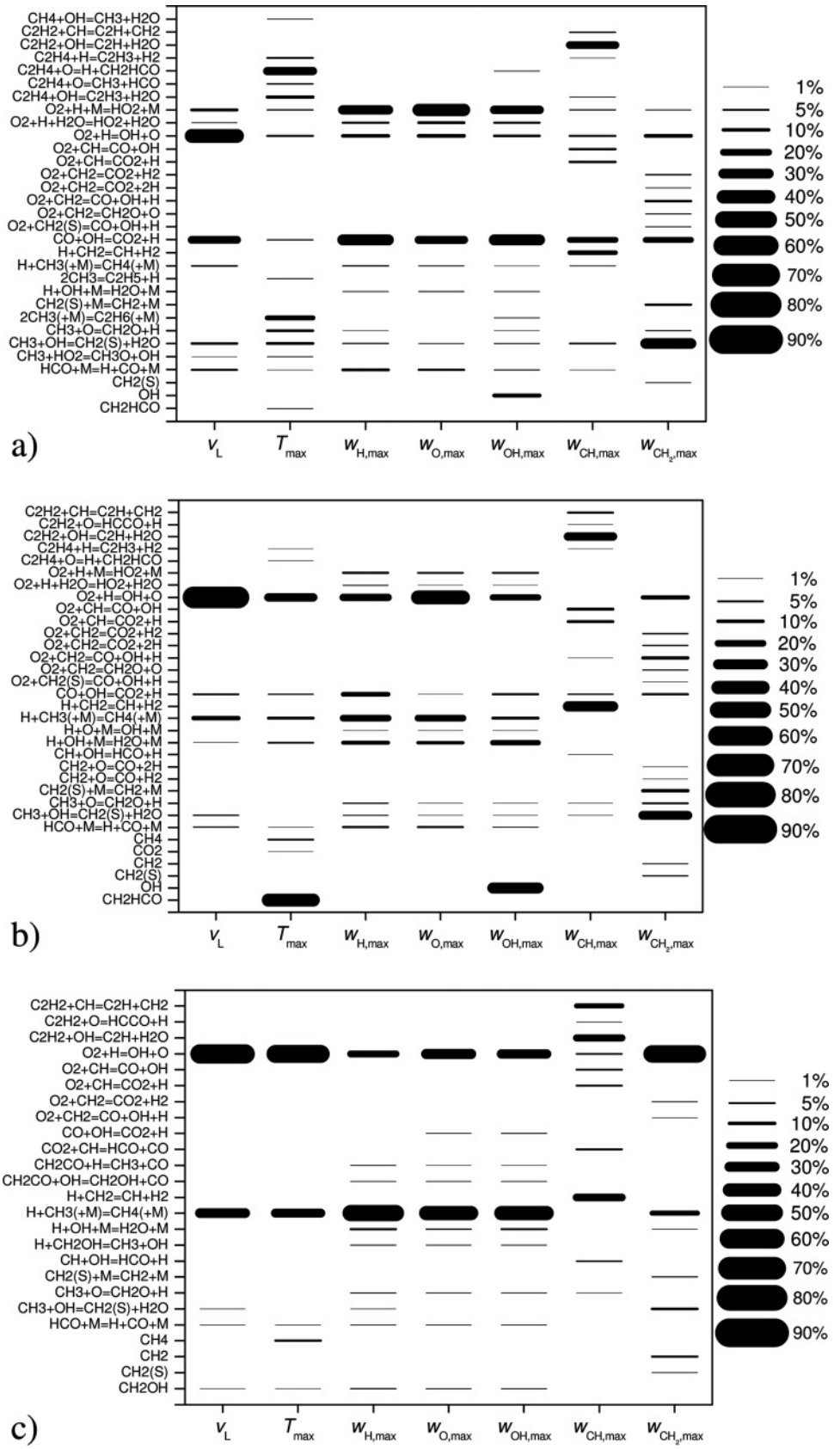

Figure 4. Percentage contributions, S_{ij}%, calculated in the local analysis are shown for those input parameters (vertical axis) which contribute at least 1% to the uncertainty of at least one monitored variable (horizontal axis). Uncertainty contributions are expressed in percentages and the greater the value, the thicker the line (continuous scale). Figures correspond to (a) lean, (b) stoichiometric, and (c) rich flames.

of rate parameters were calculated in each run. By processing the results, we obtained the global uncertainties of the local sensitivity coefficients $dY_i/d \ln k_j$; their variance, mean, and extremes were monitored for all investigated outputs and for each parameter. The results of the global uncertainty analysis of local sensitivities are presented in Figure 6. Those parameters, whose sensitivities are greater than 5% of the highest sensitivity parameter, are shown only. Only kinetic sensitivities were

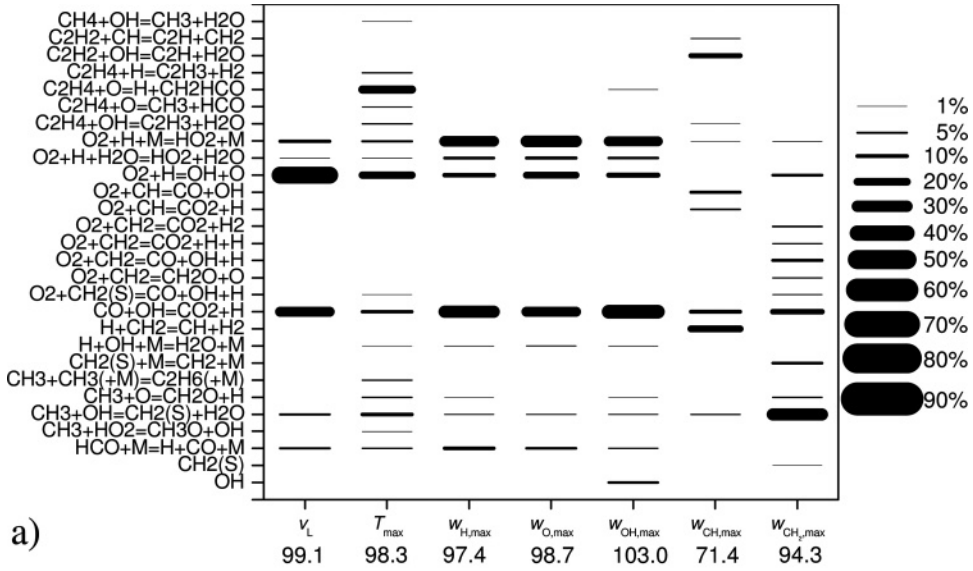

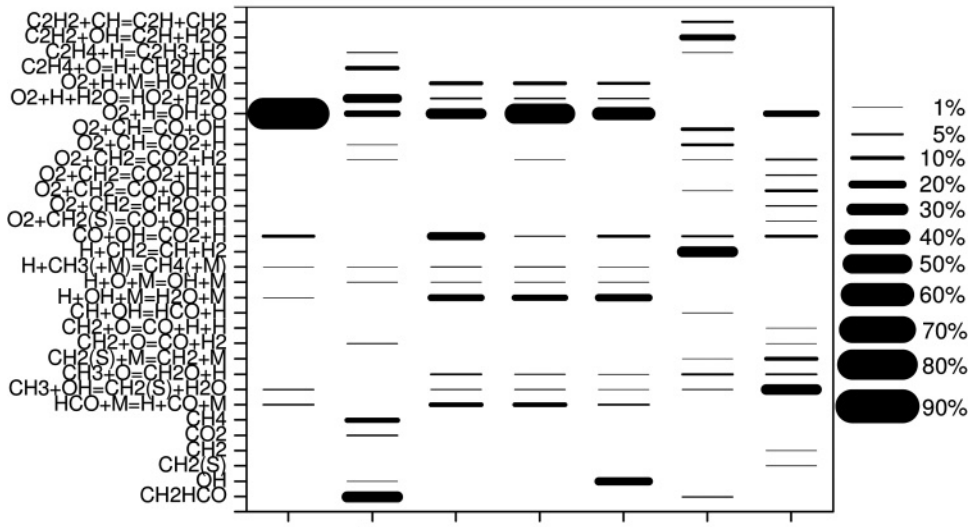

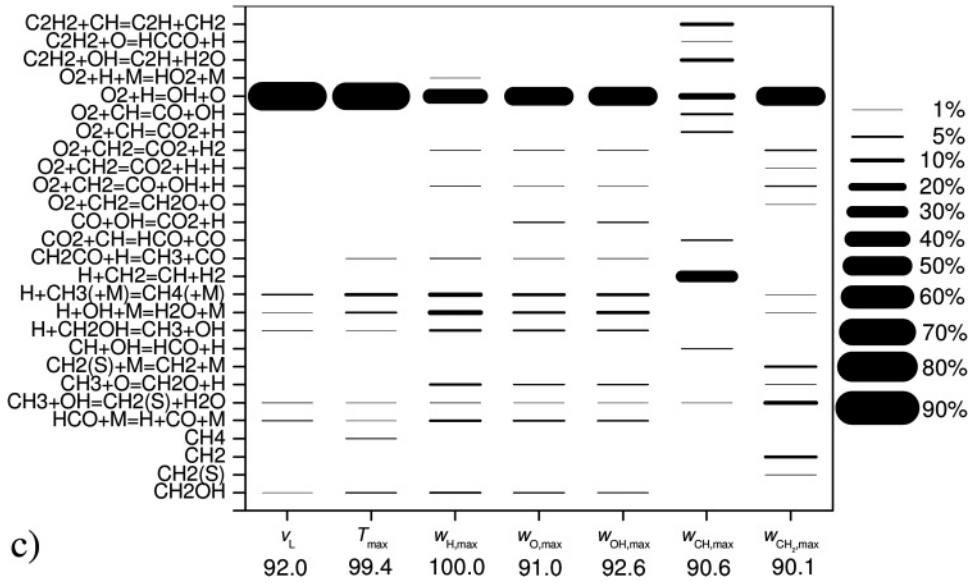

Figure 5. Speck figures created from the first-order indices $S_{j(i)}$ multiplied by 100: (a) $\varphi = 0.70$, (b) $\varphi = 1.00$, and (c) $\varphi = 1.20$. Only $S_{j(i)} > 0.01$ values are shown. Numbers below the horizontal axes are the sums of the first-order indices multiplied by 100.

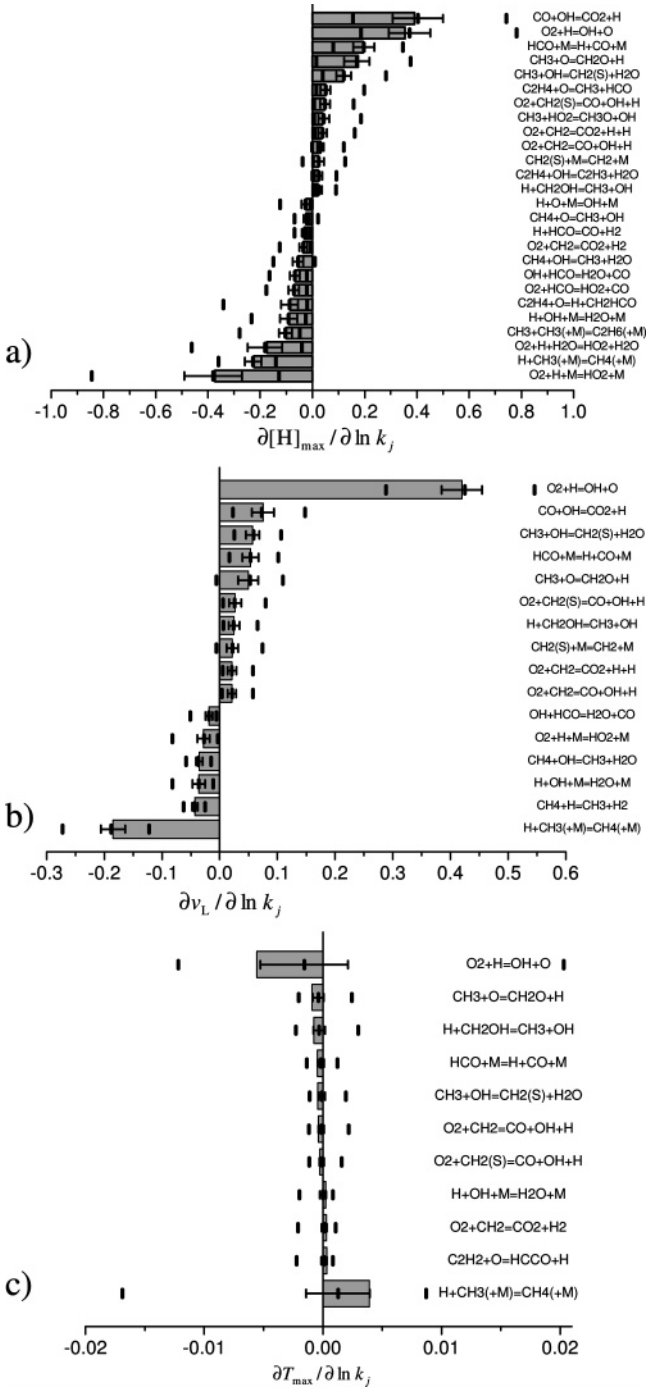

Figure 6. Result of global uncertainty analysis of the local sensitivity coefficients for (a) $w_{H,max}$ at $\varphi = 0.70$, (b) the laminar flame velocity at $\varphi = 1.00$, and (c) T_{max} at $\varphi = 1.20$. Only those reactions are shown whose rate parametric sensitivities are greater than 5% of that of the one with the highest sensitivity. Gray stripes refer to the local sensitivity coefficients at the nominal parameter set, small bars interconnected with a horizontal line indicate the 1σ uncertainty interval of local sensitivity coefficients, and outer larger bars show the attainable minimum and maximum sensitivity coefficients at any parameter set within the uncertainty limits of parameters.

investigated here because local sensitivity coefficients $\partial Y_i/\partial \ln k_j$ are usually used for kinetic analysis or mechanism reduction.

Figure 6a−c shows only some representative examples, but very similar figures were obtained for other variables and for other equivalence ratios. For the laminar flame velocity sensitivities and the maximum hydrogen atom concentration sensitivities, the 1σ uncertainty limits are relatively narrow, and the minimum and maximum achievable values span a wider range (see Figure 6a,b). Similar figures were obtained for the local sensitivity coefficients of all other concentrations. For the maximum temperature sensitivities, larger deviations were found (results for $\varphi = 1.20$ are shown in Figure 6c). Most parameters have either positive or negative sensitivity coefficients at any set of parameters. In the cases of some other parameters, the sign of the sensitivity coefficient depends on the parameter set. For example, in the case of maximum temperature (Figure 6c), all important parameters can have both positive and negative sensitivity coefficients assigned to them depending on the actual parameter set, and for the flame velocity and maximum H concentration, most sensitivity coefficients keep their signs. It was also found that the order of importance of the sensitivity functions depends on the actual parameter sets; however, within the 1σ uncertainty range, the changes in the order are minor, and the most important parameters are always the same.

TABLE 2: Comparison of the Four Methods Applied

	local	Morris	MC LHS	Sobol'
takes the variance of the parameters into account	yes	yes	yes	yes
takes the *pdf* of the parameters into account	no	no	yes	yes
provides the variance of the output	yes (biased)	no	yes	yes
provides the *pdf* of the output	no	no	yes	no
computationally cheap	yes	medium	no	no
provides contributions of individual parameters	yes	yes[a]	no[b]	yes
global method	no	yes	yes	yes
provides information on nonlinearity	no	yes[a]	no	yes
number of required simulations[c]	1	2130	3000	∼15000

[a] Qualitative information only. [b] Pearson coefficients indicate the individual parameter contributions, but such a calculation requires about 100 times more simulations than is required for the estimation of the *pdf* of the output. [c] The number of simulations for the methane flame model at each equivalence ratio, discussed in this paper.

4. Conclusions

Uncertainty analysis is important for modeling of complex reaction systems, such as combustions or atmospheric processes. It is now widely accepted that calculated uncertainty should accompany model outputs because it contains valuable information about the reliability of the results. Uncertainty analysis can also reveal whether further experimental or theoretical work is needed to get a more reliable description of these systems.

Flat, laminar, premixed methane−air flames were modeled using the Leeds methane oxidation mechanism at three equivalence ratios, and uncertainty analysis was carried out with four different methods. The advantages and drawbacks of these methods are summarized in Table 2. The *pdf*'s of the monitored outputs were established by the Monte Carlo analysis with Latin hypercube sampling. It was shown that the predicted maximum flame temperature, the laminar flame velocity, and the concentration of radicals O, H, and OH have a low uncertainty in all cases, but the concentrations of radicals CH and CH_2, important in the prompt NO_x formation, are predicted with large uncertainty. Most of the uncertainties are caused by the uncertainties in the rate coefficient of the $O_2 + H = OH + O$ reaction, although the extent of its influence was indicated slightly differently by the different methods. From the Morris and the Sobol' method, it is clear that nonlinearities should be taken into account; however, greater differences between the results of local and global methods were found only in the rich case.

The shares of the thermodynamic uncertainties are much lower than those of the kinetic ones but are not negligible in some cases. Finally, it was shown that in the investigated methane flame model the local sensitivity coefficients are robust measures of the reaction importance.

In this paper, all thermodynamic and kinetic parameters were assumed to be uncorrelated. The reason was that thermodynamic tables and kinetic data evaluations contain data on the uncertainty of each parameter, but there is no information on the correlation of them. Enthalpy of formation data can be obtained from (uncorrelated) mass spectrometric measurements, but these are deduced also from equilibrium constants, which have been determined by measuring the rate coefficients of the opposing reactions. Equilibrium constants are then converted to enthalpies of reactions, which are the sums of several enthalpies of formation. This ensures that there is a strong correlation among the enthalpies of formation of species, which is not indicated in the summary tables. The Active Table approach of Ruscic et al.[57,58] ensures not only that all recommended enthalpies of formation are consistent with each other but also that it can provide the joint *pdf* of the enthalpies of formation or at least a correlation matrix. When such information is available for all species of methane oxidation, the thermodynamic uncertainty analysis should be repeated. It was also assumed that there is no correlation between the enthalpies of formation and the kinetic parameters. This is probably true because the rate coefficients of the methane oxidation reactions are typically not used for the derivation of thermodynamic data.

Rate coefficients in the 300−500 K temperature range are usually determined by laser-flash photolysis or discharge flow methods. These measurements do not require assumptions for the values of other rate coefficients and are therefore usually uncorrelated. However, rate coefficients above 1500 K are usually determined by shock tube or flame measurements. At the evaluation of these measurements, several-step mechanisms are used and the rate coefficients of other reactions are utilized. This ensures a strong correlation among the rate coefficients of several reactions. As a result, if the rate coefficient is temperature dependent, the Arrhenius parameters of the reactions will be correlated. Such correlations are not indicated in the kinetic data evaluations.

Reaction mechanisms are traditionally assembled in such a way that the recommended rate parameters are assigned to the reaction steps. Usually, the obtained reaction mechanism does not reproduce the bulk measurements, such as flame velocities or time-to-ignition data. Then, some of the rate coefficients are tuned within the $[k_{min}, k_{max}]$ limits to achieve a better agreement. The problem is that similarly good agreement can be achieved by tuning other parameters. Note, we have shown[59−61] that in the cases of several kinetic models an infinite number of parameter sets can provide practically identical simulation results, which can be an explanation to this common observation.

An interesting outcome of our calculations was that by changing all parameters within their allowed $[k_{min}, k_{max}]$ range, all simulation results but the calculated maximal temperature could be varied in a very wide range. Selecting rate coefficients from their allowed range to reproduce all available bulk experimental data introduces a further correlation between them and a further restriction for the allowed parameter values. An in-depth discussion of this type of correlation can be found in the recent articles of Frenklach et al.[62−64]

The final conclusion is that the results presented here should be refined later when the correlation of all parameters (ideally in the form of a parametrized joint *pdf*) becomes available. All uncertainty analysis methods used here but the Morris method can be used in the present or in an extended form to handle correlated parameters. Most qualitative findings are expected to remain unchanged, but surely, the quantitative results will change when the correlations are also taken into account.

Acknowledgment. The support of OTKA T043770 and the OTKA Instrumental Grant M042110 are greatly acknowledged.

References and Notes

(1) DeMore, W. B.; Sander, S. P.; Golden, D. M.; Hampson, R. F. J.; Kurylo, M. J.; Howard, C. J.; Ravishankara, A. R.; Kolb, C. E.; Molina, M. J. *Chemical kinetics and photochemical data for use in stratospheric modeling*, evaluation number 12; JPL publication 97-4; Jet Propulsion Laboratory, 1997.

(2) Atkinson, R.; Baulch, D. L.; Cox, R. A.; Hampson, R. F.; Kerr, J. A.; Rossi, M. J.; Troe, J. *J. Phys. Chem. Ref. Data* **1999**, *28*, 191.

(3) Baulch, D. L.; Cobos, C. J.; Cox, R. A.; Esser, C.; Frank, P.; Just, T.; Kerr, J. A.; Pilling, M. J.; Troe, J.; Walker, R. W.; Warnatz, J. *J. Phys. Chem. Ref. Data* **1992**, *21*, 411.

(4) Baulch, D. L.; Cobos, C. J.; Cox, R. A.; Frank, P.; Hayman, G. D.; Just, T.; Kerr, J. A.; Murrels, T.; Pilling, M. J.; Troe, J.; Walker, R. W.; Warnatz, J. *Combust. Flame* **1994**, *98*, 59.

(5) Warnatz, J. In *Combustion chemistry*; Gardiner, W. C., Ed.; Springer: New York, 1984; p 197.

(6) *JANAF thermochemical tables, national standard reference data series*; NSRDS-NBS-37; 1971 and subsequent updates.

(7) Burcat, A. Thermochemical data for combustion calculations. In *Combustion chemistry*; Gardiner, W. C., Ed.; Springer: New York, 1984; p 455.

(8) Tsang, W. Heats of formation of organic free radicals by kinetic methods. In *Energetics of organic free radicals*; Simoes, J. A. M., Greenberg, A., Liebman, J. F., Eds.; Blackie Academic and Professional: London, 1996.

(9) Berkowitz, J.; Ellison, G. B.; Gutman, D. *J. Phys. Chem.* **1994**, *98*, 2744.

(10) Burcat, A. Ideal gas thermochemical database. ftp://ftp.technion.ac.il/pub/supported/aetdd/thermodynamics. Mirrored at http://garfield.chem.elte.hu/Burcat/burcat.html (2001).

(11) Kerr, J. A. *CRC handbook of chemistry and physics*, 78th ed.; CRC Press: Boca Raton, FL, 1997−1998.

(12) Chase, M. W. *J. Phys. Chem. Ref. Data* **1998**, *27*, I.

(13) Frenkel, M.; Marsch, K. N.; Wilbrit, R. C.; Kabo, G. J.; Roganov, G. N. *Thermodynamics of organic compounds in the gas state*; Thermodynamics Research Center: College Station, TX, 1994; Vols. I−II.

(14) Gurvich, L. V.; Veyts, I. V.; Alcock, C. B. *Thermodynamic properties of individual substances*; Hemisphere: New York, 1989; Vols. I−II.

(15) McMillen, D. F.; Golden, D. M. *Annu. Rev. Phys. Chem.* **1982**, *33*, 493.

(16) Ruscic, B.; Boggs, J. E.; Burcat, A.; Császár, A. G.; Demaison, J.; Janoschek, R.; Martin, J. M. L.; Morton, M. L.; Rossi, M. J.; Stanton, J. F.; Szalay, P. G.; Westmoreland, P. R.; Zabel, F.; Bérces, T. *J. Phys. Chem. Ref. Data* **2005**, *34*, 573−656.

(17) Burcat, A. Third millenium ideal gas and condensed phase thermochemical database for combustion; Technion Aerospace Engineering, 2001.

(18) Cox, J. D.; Wagman, D.; Medvedev, V. A. *CODATA Key Values for Thermodynamics*; Hemisphere: New York, 1989.

(19) Warnatz, J. *Proc. Combust. Inst.* **1992**, *24*, 553.

(20) Bromly, J. H.; Barnes, F. J.; Muris, S.; You, X.; Haynes, B. S. *Combust. Sci. Technol.* **1996**, *115*, 259.

(21) Brown, M. J.; Smith, D. B.; Taylor, S. C. *Combust. Flame* **1999**, *117*, 652.

(22) Turányi, T.; Zalotai, L.; Dóbé, S.; Bérces, T. *Phys. Chem. Chem. Phys.* **2002**, *4*, 2568.

(23) Phenix, B. D.; Dinaro, J. L.; Tatang, M. A.; Tester, J. W.; Howard, J. B.; McRae, G. J. *Combust. Flame* **1998**, *112*, 132.

(24) Reagan, M. T.; Najm, H. M.; Ghanem, R. G.; Knio, O. M. *Combust. Flame* **2003**, *132*, 545.

(25) Tomlin, S. A. *Reliab. Eng. Syst. Saf.* **2005**, in press.

(26) Zsély, I. G.; Zádor, J.; Turányi, T. *Proc. Combust. Inst.* **2005**, *30*, 1273.

(27) Stolarski, R. S.; Butler, D. M.; Rundel, R. D. *J. Geophys. Res.* **1978**, *83*, 3074.

(28) Derwent, R. G.; Hov, O. *J. Geophys. Res.* **1988**, *93*, 5185.

(29) Raes, F.; Saltelli, A.; Van Dingenen, R. *J. Aerosol Sci.* **1992**, *23*, 759.

(30) Saltelli, A.; Hjorth, J. *J. Atmos. Chem.* **1995**, *21*, 187.

(31) Campolongo, F.; Tarantola, S.; Saltelli, A. *Comput. Phys. Commun.* **1999**, *117*, 75.
(32) Gao, D. F.; Stockwell, W. R.; Milford, J. B. *J. Geophys. Res., [Atmos.]* **1996**, *101*, 9107.
(33) Thompson, A. M.; Stewart, R. W. *J. Geophys. Res., [Atmos.]* **1991**, *96*, 13089.
(34) Gao, D. F.; Stockwell, W. R.; Milford, J. B. *J. Geophys. Res., [Atmos.]* **1995**, *100*, 23153.
(35) Carslaw, N.; Jacobs, P. J.; Pilling, M. J. *J. Geophys. Res., [Atmos.]* **1999**, *104*, 30257.
(36) Hanna, S. R.; Chang, J. C.; Fernau, M. E. *Atmos. Environ.* **1998**, *32*, 3619.
(37) Wang, L.; Milford, J. B.; Carter, W. P. L. *Atmos. Environ.* **2000**, *34*, 4337.
(38) Wang, L.; Milford, J. B.; Carter, W. P. L. *Atmos. Environ.* **2000**, *34*, 4349.
(39) Zádor, J.; Wagner, V.; Wirtz, K.; Pilling, M. J. *Atmos. Environ.* **2005**, *39*, 2805.
(40) Moulika, M. D.; Milford, J. B. *Atmos. Environ.* **1999**, *33*, 869.
(41) Considine, D. B.; Stolarski, R. S.; Hollandsworth, S. M.; Jackman, C. H.; Fleming, E. L. *J. Geophys. Res., [Atmos.]* **1999**, *104*, 1749.
(42) Rodrigez, M. A.; Dabdub, D. *J. Geophys. Res., [Atmos.]* **2003**, *108*, No. *4443*.
(43) Turányi, T.; Hughes, K. J.; Pilling, M. J.; Tomlin, S. A. Combustion simulations at the Leeds University and at the ELTE. http://garfield-.chem.elte.hu/Combustion/Combustion.html and http://www.chem.leeds.ac.uk/Combustion/Combustion.html (2005).
(44) *Sensitivity analysis*; Saltelli, A., Scott, E. M., Chen, K., Eds.; Wiley: Chichester, 2000.
(45) Morris, M. D. *Technometrics* **1991**, *33*, 161.
(46) Campolongo, F.; Cariboni, J.; Saltelli, A. *Reliab. Eng. Syst. Saf.*, in press.
(47) Saltelli, A. *Comput. Phys. Commun.* **2002**, *145*, 280.
(48) Sobol', I. M. *Mater. Modell.* **1990**, *2*, 112.
(49) Saltelli, A.; Tarantola, S.; Chan, K. *Technometrics* **1999**, *41*, 39.
(50) Herbon, J. T.; Hanson, R. K.; Golden, D. M.; Bowman, C. T. *Proc. Combust. Inst.* **2002**, *29*, 1201.
(51) Ruscic, B.; Feller, D.; Dixon, D. A.; Peterson, K. A.; Harding, L. B.; Asher, R. L.; Wagner, A. F. *J. Phys. Chem. A* **2001**, *105*, 1.
(52) Kee, R. J.; Grcar, J. F.; Smooke, M. D.; Miller, J. A. *A FORTRAN program for modeling steady laminar one-dimensional premixed flames*; Sandia National Laboratories, 1985.
(53) Turányi, T. *KINALC: Program for the analysis of gas kinetic systems*, 1.7 ed.; 2002.
(54) Hughes, K. J.; Turányi, T.; Clague, A. R.; Pilling, M. J. *Int. J. Chem. Kinet.* **2001**, *33*, 513.
(55) Bosschaart, K. J.; de Goey, L. P. H. *Combust. Flame* **2003**, *132*, 170. Bosschaart, K. J.; de Goey, L. P. H. *Combust. Flame* **2004**, *136*, 261.
(56) Morbidelli, M.; Wu, H. *Parametric sensitivity in chemical systems*; Cambridge University Press: Cambridge, NY; 1999.
(57) Ruscic, B.; Pinzon, R. E.; Morton, M. L.; von Laszevski, G.; Bittner, S. J.; Nijsure, S. G.; Amin, K. A.; Minkoff, M.; Wagner, A. F. *J. Phys. Chem. A* **2004**, *108*, 9979.
(58) Ruscic, B.; Litorja, M.; Asher, R. L. *J. Phys. Chem. A* **1999**, *103*, 8625.
(59) Zsély, I. G.; Zádor, J.; Turányi, T. *J. Phys. Chem. A* **2003**, *107*, 2216.
(60) Zádor, J.; Zsély, I. G.; Turányi, T. *Int. J. Chem. Kinet.* **2004**, *36*, 238.
(61) Zsély, I. G.; Zádor, J.; Turányi, T. *Combust. Theory Modell.*, in press.
(62) Frenklach, M.; Packard, A.; Seiler, P. Prediction uncertainty from models and data. Presented at the American Control Conference, Anchorage, AK, 2002.
(63) Frenklach, M.; Packard, A.; Seiler, P.; Feeley, R. *Int. J. Chem. Kinet.* **2004**, *36*, 57.
(64) Feeley, R.; Seiler, P.; Packard, A.; Frenklach, M. *J. Phys. Chem. A* **2004**, *108*, 9573.